Analytical and Bioanalytical Chemistry (2020) 412:3891–3902
https://doi.org/10.1007/s00216-019-02308-w

RESEARCH PAPER

Continuous flow separation of particles with insulator-based dielectrophoresis chromatography

Nicole Hill[1] · Blanca H. Lapizco-Encinas[1]

Received: 11 October 2019 / Revised: 15 November 2019 / Accepted: 27 November 2019 / Published online: 2 January 2020

Abstract

The development of insulator-based dielectrophoresis chromatography is proposed here as a novel hybrid technique that capitalizes on the simplicity of insulator-based dielectrophoresis (iDEP) and the well-known chromatographic theory. Chromatographic parameters are employed to characterize dielectrophoretic separation of particles with particles being eluted from the system as enriched particle *peaks*. By varying the characteristics of the insulating posts, it was possible to manipulate the *interactions* of the particles with the insulating post array which acted as the *stationary phase*. The present work studied how the characteristics of the particles affected the *particle retention*. Different types of particles have distinct interactions with the post array; these interactions depend on particle properties (size, electrical charge, and polarizability). This work includes mathematical modeling with COMSOL and extensive experimentation. Particles ranging from 1 to 10 μm in diameter were tested for retention time and eluted as peaks in the iDEP chromatography devices. Separation results were reported in the form of dielectropherograms including the estimation of retention time (t_R), separation efficiency (N/meter), and separation resolution (R_s). Two full separations were demonstrated: a separation by charge between two types of particles of similar size (~ 10 μm) with different electrical surface charges and a separation by size between 2- and 5-μm particles with similar surface charge (difference in ζ_P of 4 mV). The achieved separation resolutions were $R_s = 1.8$ and $R_s = 3.5$, respectively. This is the first study on DEP chromatography to assess performance in terms of resolution and separation efficiency, demonstrating the unique potential of iDEP chromatography.

Keywords Dielectrophoresis · Chromatography · Electrophoresis · Electrokinetics · Microfluidics · Microparticles

Introduction

Microfluidic technologies have revolutionized many analytical applications allowing for rapid sorting, enrichment, and separation of target particles and cells. Some of the benefits of microscale assessments include smaller sample volumes, faster processing, and high resolution and sensitivity [1]. Electric field–driven techniques, also known as electrokinetic (EK) techniques, such as electroosmosis (EO), electrophoresis (EP), and dielectrophoresis (DEP) have been shown to be especially prominent in microfluidics [2].

Dielectrophoresis has gained significant attention during the last 15 years as a technique with great flexibility that can be used over a wide array of configurations [3, 4]. Dielectrophoresis is defined as particle motion due to exposure to a non-uniform electric field, allowing for particles to move according to their relative polarity with the media. Particles can either be attracted to areas of greater electric field strength (positive DEP, pDEP) or repulsed (negative DEP, nDEP). Dielectrophoresis does not rely on particle charge to operate. There are two main application modes of DEP: electrode-based DEP (eDEP) and insulator-based DEP (iDEP). The former is more established, as DEP was discovered with an eDEP system [5]. The latter is a more recent technique that requires simpler and more robust systems, since non-uniform electric fields are created by the presence of insulating structures, commonly known as posts [6].

Published in the topical collection *Bioanalytics and Higher Order Electrokinetics* with guest editors Mark A. Hayes and Federica Caselli.

Electronic supplementary material The online version of this article (https://doi.org/10.1007/s00216-019-02308-w) contains supplementary material, which is available to authorized users.

✉ Blanca H. Lapizco-Encinas
bhlbme@rit.edu

[1] Microscale Bioseparations Laboratory, Biomedical Engineering Department, Rochester Institute of Technology, Institute Hall (Bldg. 73), 160 Lomb Memorial Drive, Rochester, NY 14623-5604, USA

Insulator-based DEP has been proven to be an effective technique for particle separation, enrichment, and sorting, including submicron particles such as proteins [7–9], DNA [10, 11], organelles [12, 13] and viruses [14], and cells [15, 16] and parasites [17]. Understanding how to optimize the design of iDEP devices is critical, and numerous research groups around the world have devoted significant effort to the optimization of iDEP devices. Several studies have been reported on optimizing insulating post shape and arrangement to increase particle trapping in iDEP devices. Kwon et al. [18] explored simulations of different insulating post shapes and spacing to maximize particle trapping with pDEP. A 2013 study from our group explored the effects of post shapes (circle and diamond) on the distribution of the gradient of the electric field to enhance nDEP forces on particles and promote particle trapping [19]. The work was expanded in 2014 by exploring narrower and wider post shapes, where narrower posts produced better particle trapping [20]. A more recent report by our group was focused on optimizing post arrangement (longitudinal and latitudinal spacing) to decrease the required voltage to achieve particle trapping with nDEP [21]. Pesch et al. [22] performed a detailed model considering the polarization of the insulating posts and focused on enhancing DEP particle trapping. Another recent study showed that there is an optimal post radius for a given vertical spacing that maximizes the electric field gradient to enhance nDEP effects on particles [23]. The studies listed above illustrate some of the latest findings on the optimization of post shape and arrangement for particle trapping with iDEP.

Several well-established chromatographic techniques relying on the use of electric fields have been developed, including electrochemically modulated liquid chromatography [24, 25], capillary electrochromatography [24, 26, 27], and micellar electrokinetic chromatography [27, 28]. However, dielectrophoretic chromatography has only been studied by a few groups: Holmes and Morgan [29], the Washizu group [30–32], and more recently, the Agah group [33] and Giesler et al. [34]. All of these studies employed eDEP systems. Holmes and Morgan employed an eDEP design with two systems of electrodes. Cells were first focused to the channel center with nDEP with the first electrode system, followed by cell attraction by means of pDEP at the second electrode system. Depending on their characteristics (size and dielectric properties), cells followed distinct trajectories and were retained at locations in the second electrode system. No dielectropherogram or separation resolution was reported [29]. The Washizu group also developed an eDEP chromatography system with interdigitated electrodes that were used to trap biomolecules and perform separations by size [30–32]. One of their systems had a constant fluid flow velocity; an electrical field was applied and particles were trapped by pDEP. Larger particles had a greater probability of trapping while smaller molecules continued flowing through the system with minimum interference. The electric field was turned off in order to release the particles and obtain a dielectropherogram of fluorescence vs. time. System performance was assessed in terms of collection ratio [31]. Their last report [32], which featured cross flow, included well-defined dielectropherograms for the separation of two types of DNA molecules (6.6 kbp and 48.5 kbp); however, separation resolution was not reported. Work by the Agah group [33] employed a combination of insulating posts and embedded electrodes to create a device with a focusing region, followed by a separation region with tunable electric fields utilizing AC signals to selectively trap submicron particles. Giesler et al. [34] utilized an eDEP technique in which micron-sized particles are separated by their DEP mobility. Particles with higher DEP mobility have a stronger attraction to the electrodes and are pulled and temporarily immobilized, whereas particles with lower DEP mobilities are able to pass through the system faster and are not delayed as often by the pull of the electrodes.

There are numerous reports on particle manipulation and enrichment with trapping iDEP [21, 35, 36]. The technique presented here, however, is based on streaming iDEP. Trapping iDEP is when DEP is the dominant force present in the system and particles can be captured and enriched with DEP. Streaming iDEP is a hybrid dielectrophoretic regime where particle migration is controlled by both linear EK and DEP; i.e. DEP is not the dominant force in the system [36, 37]. Streaming iDEP has been successfully demonstrated as a sorting technique in curvature-induced DEP [38]. The new technique proposed here merges iDEP with some of the fundamentals of chromatographic theory, such as retention time, resolution, and number of plates; we have termed this new methodology "iDEP chromatography" (iDEP-Chroma). This scheme exploits an iDEP device with a long post array that serves as the *stationary phase* (Fig. 1); particles passing through the iDEP channel *interact* with the post array. Each type of particle has a distinct *affinity* for the post array, dictated by particle properties and the characteristics of the post array. The goal of iDEP-Chroma is to maximize particle discrimination (i.e., differences in retention time) as distinct types of particles travel down the post array under streaming iDEP. A recent study by our group employed an iDEP channel with asymmetric posts [39]. The asymmetric post shape combined with a custom direct current (DC)-biased step AC waveform created a *check valve* effect for large particles. Yeast cells were successfully enriched and eluted from the system while 1-μm polystyrene particles remained inside the post array. Some of the findings obtained with the asymmetric post scheme were applied for designing the iDEP-Chroma devices presented here. Another relevant study on streaming iDEP was presented by Luo et al. [13] which utilized absolute negative mobility (ANM)—the concept that particles can move in the opposite direction as the driving force due to a periodic stimulus developed by an AC signal. Their findings demonstrated that larger particles resulted in ANM migration while smaller exhibited normal migration patterns. This scheme was demonstrated with mitochondria subjected to a DC-biased AC waveform.

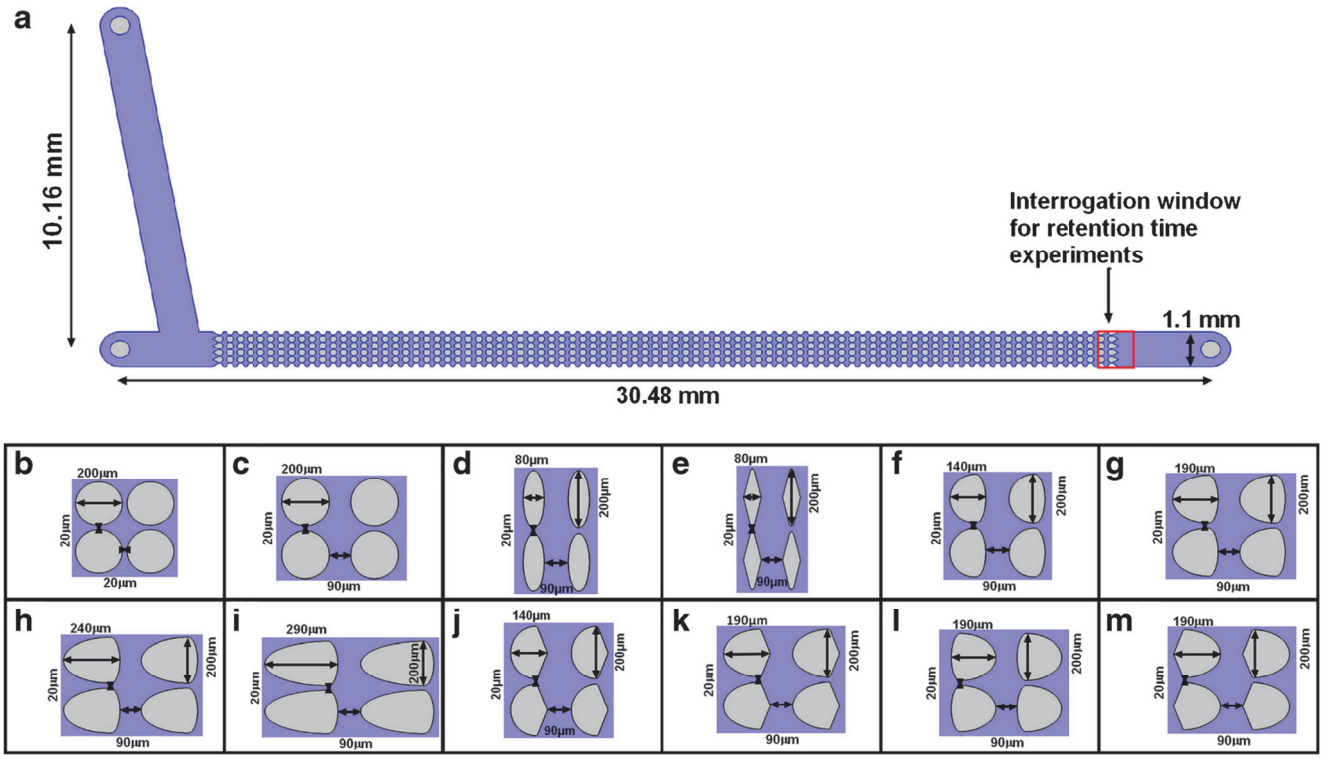

Fig. 1 Schematic representation of the microchannel designs employed for $t_{R,e}$ determination. (**a**) Illustration of a full channel with reservoirs for design "Circle-200 HS-90." For all twelve designs, an illustration of four insulating posts is included: (**b**) Circle-200 HS-20, (**c**) Circle-200 HS-90, (**d**) Oval-200-80, (**e**) Diamond-200-80, (**f**) Oval-100-Oval-40, (**g**) Oval-150-Oval-40, (**h**) Oval-200-Oval-40, (**i**) Oval-250-Oval-40, (**j**) Oval-100-Diamond-40, (**k**) Oval-150-Diamond-40, (**l**) Oval-40-Oval-150, (**m**) Diamond-40-Oval-150

The present work includes extensive simulations using COMSOL Multiphysics® to assess the influence of post shape on the streaming behavior of the particles under linear EK and DEP effects. Specific modeling parameters are included in Table S1 in the Electronic Supplementary Material (ESM). Simulation results allowed for identifying prime candidates for particle separations, one of which was tested experimentally with ten distinct types of particles. Experimental trials tracking particle retention time through the post array were used to fine tune simulation results and identify optimal geometries for different types of particle separations. Finally, two separations schemes, one exploiting particle charge differences and one exploiting particle size differences, were used to demonstrate the potential of iDEP-Chroma as a new scheme for particle separations. The parameters of separation resolution (R_s) and separation efficiency (N/meter) were employed to assess separation performance. While traditional chromatographic techniques are limited to nano-sized particles such as proteins, the ultimate goal of iDEP chromatography is to offer an alternative for the separation of micron-sized particles.

Theoretical background

Particles within an iDEP channel are subjected to two main forces: linear EK and DEP. The former is a superposition of EO and EP, which are directly proportional to the electric field

$$\vec{v}_{EK} = \mu_{EK}\vec{E} = (\mu_{EO} + \mu_{EP})\vec{E} = -\frac{\varepsilon_m(\zeta_W - \zeta_P)}{\eta}\vec{E} \quad (1)$$

$$\vec{v}_{EO} = -\frac{\varepsilon_m \zeta_W}{\eta}\vec{E} \quad (2)$$

$$\vec{v}_{EP} = \frac{\varepsilon_m \zeta_P}{\eta}\vec{E} \quad (3)$$

where μ_{EK}, μ_{EO}, and μ_{EP} refer to the electrokinetic, electroosmotic, and electrophoretic mobilities, respectively; η is the viscosity of media; and ζ_W and ζ_P are the zeta potential of the polydimethylsiloxane (PDMS) substrate and the particle, respectively. The dielectrophoretic force exerted on a spherical particle is defined as

$$\vec{F}_{DEP} = 2\pi\varepsilon_m r_p^3 Re\,(f_{CM})\nabla E^2 \quad (4)$$

where $Re(f_{CM})$ refers to the real part of the Clausius-Mossotti factor, which describes particle polarizability with respect to that of the suspending media. Under low frequency and direct current potentials, f_{CM} becomes [40]

$$f_{CM} = \left(\frac{\sigma_p - \sigma_m}{\sigma_p + 2\sigma_m}\right) \quad (5)$$

where σ_p and σ_m are the conductivity of the particle and the medium, respectively. For spherical particles, the magnitude of the f_{CM} ranges from −0.5 to 1.0 [40]. Particle charge is related to σ_p, since ζ_P influences the surface conductance (K_s) of a particle, which, in turn, modifies σ_p and f_{CM}

$$\sigma_p = \sigma_{Bulk} + \frac{K_S}{r_p} \tag{6}$$

The dielectrophoretic velocity of a particle is

$$\vec{v}_{DEP} = \mu_{DEP}\nabla E^2 = \frac{r_p^2 \varepsilon_m}{3\eta} Re[f_{CM}]\nabla E^2 \tag{7}$$

where μ_{DEP} is the dielectrophoretic mobility. All particles in this study possess a negative charge; therefore, their electrophoretic motion is toward the inlet (opposite to EO). However, since in all cases $|\zeta_W| > |\zeta_P|$ ($\zeta_W = -97.3$ mV, Table 1 contains all values of ζ_P), all particles in this study experienced a net EK motion toward the channel outlet. Due to their large size, from 1 to 10 μm, all particles in this study experienced nDEP [41, 42]. The total particle velocity considering linear EK and DEP becomes

$$\vec{v}_P = \mu_{EK}\vec{E} + \mu_{DEP}\nabla E^2 = \vec{v}_{EK} + \vec{v}_{DEP} \tag{8}$$

Three distinct flow regimes occur in iDEP channels, depending on the strength of the electric field: EK flow, streaming iDEP flow, and trapping DEP flow [37, 43]. The flow of interest for iDEP-Chroma is the streaming iDEP flow. Within this regime, DEP is comparable to the EK force but does not dominate particle migration. Under these conditions, the following expression is valid [18]:

$$\vec{J} = C_P\left(\vec{v}_{EK} + \vec{v}_{DEP}\right) = C_P\left(\mu_{EK}\vec{E} + \mu_{DEP}\nabla E^2\right) \tag{9}$$

where C_P represents the particle concentration in the suspending medium and $\vec{j}$ refers to the particle flux. For EK flow and streaming iDEP flow, particles migrate along with electric field lines, thus

$$\vec{J}\cdot\nabla\vec{E} = C_P\left(\vec{v}_{EK} + \vec{v}_{DEP}\right)\cdot\nabla\vec{E} \tag{10}$$

Rearranging Eq. (10), it is possible to obtain the condition for streaming iDEP flow, which is the primary separation mechanism employed in this work [18]

$$\left(\mu_{EK}\vec{E} + \mu_{DEP}\nabla E^2\right)\cdot\nabla\vec{E} = 0 \tag{11}$$

$$\frac{\mu_{DEP}\nabla E^2\cdot\nabla\vec{E}}{\mu_{EK}\vec{E}\cdot\nabla\vec{E}} \le -1 \tag{12}$$

In iDEP-Chroma, the potential for particle separation is based on differences in retention time (t_R), which measures how long it takes for particles to traverse the post array. The optimal iDEP design will maximize differences in t_R between particles. Retention time is calculated as

$$t_R = \left(\frac{LC\cdot NC}{\vec{v}_p}\right) \tag{13}$$

where LC is the length of one constriction and NC is the total number of columns of posts (varies for each design, see Table S2 in the ESM). An average value of $\vec{v}_p$, at the center of the constriction (see red line in the insets in Fig. 2), estimated with COMSOL was used for t_R calculations. COMSOL simulations of DEP particle behavior often require the use of a particle correction factors as has been well reported.

Table 1 Experimental simulation results for particle retention time, correction factor, and number of plates

No.	Particle, brand, color, funct.	ζ_P (mV)	Simulated t_R (s)	Experimental $t_{R,e}$ (s)	Separation efficiency (N/m)	C
1	1.1 μm, Mag, green, NF	−61.4	41.8	43.9 ± 2.0	3968 ± 584	171.0
2	2.0 μm, Mag, green, NF	−39.4	25.9	72.3 ± 10.5	1890 ± 156	149.0
3	2.0 μm, Mag, red, Car	−57.5	32.1	35.1 ± 2.9	7734 ± 1405	84.0
4	2.0 μm, Mag, green, Car	−63.8	44.8	61.9 ± 5.1	3865 ± 622	81.0
5	5.0 μm, Mag, red, Car	−53.8	34.5	40.4 ± 4.1	24,799 ± 3617	15.0
6	5.0 μm, Mag, green, NF	−61.7	42.1	45.0 ± 1.8	20,459 ± 797	9.1
7	6.8 μm, Mag, green, Car	−50.0	31.7	35.2 ± 2.5	8671 ± 1621	8.0
8	7.6 μm, Mag, green, Car	−12.4	22.6	42.9 ± 1.9	61,934 ± 2964	15.1
9	9.7 μm, Mag, green, Car	−30.8	17.7	52.7 ± 6.8	27,656 ± 7178	7.3
10	10.0 μm, Inv, red, Car	−72.6	72.7	100.4 ± 3.3	153,724 ± 9226	2.5

Correction factors were identified by matching retention time experiments with COMSOL simulations employing design Circle-200 HS-90 under 900 V
Mag Magsphere, *Inv* Invitrogen, *Car* carboxyl, *NF* non-functionalized

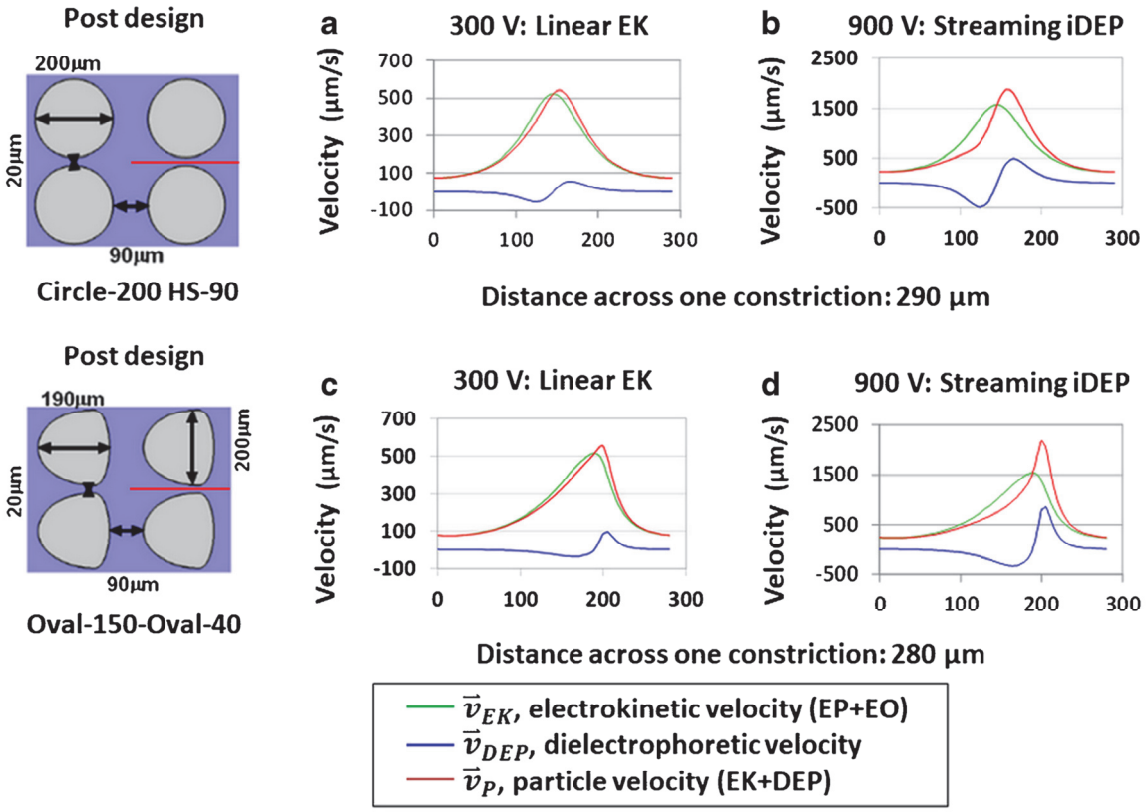

Fig. 2 Prediction of the velocity of 10-μm red carboxylated particles ($\zeta_P = -72.6$ mV) across one constriction for two distinct designs under 300 V and 900 V. (**a**, **b**) Design Circle-200 HS-90. (**a**) Linear EK-dominated regime (300 V), indicated by the similarity between the EK velocity (green) and the total velocity (red). (**b**) Streaming iDEP regime (900 V), where the total particle velocity (red) is now influenced by the DEP velocity (blue). (**c**, **d**) Design Oval-150-Oval-40, behavior is similar to the symmetric design. (**c**) Linear EK dominates at 300 V. (**d**) Streaming iDEP regime dominates at 900 V. For all cases, particle velocity was predicted along the red cutline depicted in the insets

Correction factors mainly depend on particle properties, most notably size [44]. The correction factor is usually a multiplier that modifies $\vec{v}_{DEP}$. Weiss et al. [45] measured experimentally the μ_{DEP} for 1-μm polystyrene particles to be on the order of 1×10^{-16} m^4 V^{-2} s^{-1}, approximately 4 orders of magnitude higher than those predicted by COMSOL simulations. This discrepancy clearly illustrates the need of some correction factor to help bridge the gap between experiments and simulations. The experimental retention time ($t_{R,e}$) for each particle type was used for estimating the correction factor (C) using the following expressions:

$$\vec{v}_P = \frac{LC \cdot NC}{t_{R,e}} = \vec{v}_{EK} + C \cdot \vec{v}_{DEP} \tag{14}$$

$$C = \frac{\left(\frac{LC \cdot NC}{t_{R,e}} - \vec{v}_{EK}\right)}{\vec{v}_{DEP}} \tag{15}$$

For comparison to well-established separation techniques, such as chromatography and capillary electrophoresis, the experimental results were evaluated in terms of the number of plates (N) and resolution (R_s), which depend on $t_{R,e}$, and peak width (W). Separation efficiency (N/meter) was estimated by dividing N by device length.

$$N = \frac{16\, t_{R,e}{}^2}{W^2} \tag{16}$$

$$R_s = \frac{2\left(t_{R2,e} - t_{R1,e}\right)}{W_1 + W_2} \tag{17}$$

Experimental section

Microdevices, particles, and suspending media

PDMS was used to create microchannels containing arrays of insulating posts by employing standard soft lithography techniques as reported by our group [39, 46]. The microchannels were either 30.48 mm or 51.54 mm long, 1.1 mm wide, and 40 μm deep. All post array designs are shown in detail in Fig. 1. Ten different fluorescent particle suspensions were made of varying concentrations (7.2×10^4–1.8×10^9 particles/mL); these particles were purchased from two providers: Invitrogen (Eugene, OR) and Magsphere (Pasadena, CA). The

chosen microspheres vary in size, surface functionalization, and electrical charge (see Table 1). Particle image velocimetry was used to determine ζ_P values [47, 48]. The suspending medium was deionized water with Tween 20 (0.05% v/v) and 0.1 M KOH added to adjust the medium conductivity to 15–25 μS/cm and pH to 6.0–6.5. Media properties, pH and conductivity, were carefully selected, since they influence both DEP and EK phenomena. Low-conductivity medium produces higher EK velocities, and higher medium pH increases the EK velocity as well in the case of negatively charged substrates [49], which is the case for PDMS. As streaming conditions are required for this separation technique, particle trapping was avoided by employing a low-conductivity medium and maintaining the pH of media above 6.0. Regarding DEP, the conductivity of media affects particle conductivity (since it alters particle surface conductance [50]) and the magnitude of the Clausius-Mossotti factor (Eq. (5)). However, under the experimental conditions of this study, the conductivity of the polystyrene particles is significantly less than that of the suspending media, meaning there should not be an appreciable change in particle DEP response with slight variances in pH or conductivity [51]. The properties of suspending media were kept relatively constant throughout the experiments to minimize any changes in zeta potentials of the particles and the channel walls. This medium generates an approximate $\zeta_W = -97.3$ mV in our PDMS devices.

Equipment and experimental procedure

Microparticles were visualized and recorded as videos with a Zeiss Axiovert 40 CFL inverted microscope (Carl Zeiss Microscopy, Thornwood, NY). DC electric potentials were applied with a high voltage supply (HVS6000D, LabSmith, Livermore, CA) using platinum electrodes.

Results and discussion

Linear EK vs. streaming iDEP regimes

The first objective was establishing the required voltages for achieving sufficient streaming iDEP particle behavior while avoiding particle trapping [36]. Streaming iDEP is when linear EK and DEP are comparable and particles migrate under the influence of both forces [37]. In an iDEP device (Fig. 1a), as a particle approaches a constriction between two insulating posts, DEP effects appear and vary depending on particle position. Figure 2 illustrates predicted particle velocities across one constriction for two distinct post shapes: symmetric and asymmetric. Particles are repelled upstream by DEP prior to the constriction (negative direction) and are pushed downstream by DEP after the constriction (positive direction). Figure 2a–d (blue line) illustrates how the $\vec{v}_{DEP}$ has a negative and positive region. Furthermore, linear EK migration also varies as the electric field is higher at the constriction, producing a maxima for $\vec{v}_{EK}$ at the constriction center (Fig. 2a–d, green line). As seen in Figure 2, DEP slows particles down while linear EK accelerates particles up as they approach each constriction; then, once the particles have crossed the constriction center, both forces accelerate the particles. The combination of these two forces yields the total particle velocity ($\vec{v}_P$) which is represented by the red line in Fig. 2a–d.

Figure 2 allows comparing the magnitudes of linear EK and streaming iDEP regimes. At the lower voltage of 300 V (Fig. 2a, c), DEP is too weak to make an appreciable impact and particle movement is dictated almost entirely by linear EK; this is an example of linear EK regime. At the higher voltage of 900 V (Fig. 2b, d), DEP now makes a significant impact on particle behavior, and both DEP and linear EK are influencing particle movement, illustrating the streaming iDEP regime. An attractive characteristic of the iDEP-Chroma scheme is that we can separate particles by size and charge differences, since linear EK (depends on charge) and DEP (depends in size and polarizability) are both influencing particle movement.

Figure 2 also compares the distinct particle behavior obtained with symmetrical (Fig. 2a, b, circle) and asymmetrical (Fig. 2c, d, Oval-150-Oval-40) insulating posts. The use of asymmetric posts produces a *skewed* particle velocity as the particle crosses a constriction region. In this case, the asymmetric posts have their *shorter side* toward the outlet, enhancing particle acceleration as the particle exits the constriction. Since this acceleration is dictated by DEP, it depends on particle size and polarization, making it distinct for each one of the ten particles employed here. The post asymmetry allows better discrimination of particles, as different particles will experience a distinct level of acceleration forward as they cross each one of the constrictions in the long post arrays employed in this study. The strategic use of asymmetric post shapes and streaming regime in iDEP-Chroma is illustrated in the next sections.

Estimating correction factors for improved model predictions

Microchannels with the post array from Fig. 1c were utilized to assess experimental particle retention time ($t_{R,e}$); i.e., how long the particles needed to traverse the post array which acted as the stationary phase. These results are listed in Table 1. Multiple trials on multiple channels were performed to ensure reproducibly of particle behavior.

Correction factors are commonly employed to improve the accuracy of mathematical models in iDEP [44]. As the primary feature of interest in the simulations, retention time was used as the basis for estimating correction factors. The correction factors (C) in Table 1 were obtained by matching the

experimental retention time ($t_{R,\ e}$) to the predicted retention time (t_R) for each particle type, employing Eq. (14). Under an applied voltage of 900 V, particles migrated through the post array. The time of peak fluorescence intensity at the end of the post array from the initial elution of particle was used to represent $t_{R,\ e}$. Different correction factors were tested, modifying the dielectrophoretic velocity in the models in such a way that the predicted t_R matched $t_{R,\ e}$. One clear trend emerges from Table 1: the easier a particle is to trap, the lower the needed correction factor. Particle trapping is inherently dependent on particle size; i.e., larger particles need a lower correction value. However, for particles of similar size, another parameter emerges: zeta potential of the particle. Particles with zeta potentials that are of a greater negative magnitude have a higher competition between EO and EP. This yields a lower overall EK velocity, making it easier to for DEP to trap the particles. One particle illustrates this idea most clearly: the 7.6-μm particles (particle no. 8 in Table 1, $\zeta_P = -12.4$ mV). This particle breaks the pattern with correction factors if only size is a factor as the 7.6-μm particles have a correction factor of 15.1. However, the extremely low zeta potential of the 7.6-μm particles means they provide almost no impediment to the EO velocity and so move very quickly through the system, making them hard to trap despite their large size. Particle size and charge are explored to identify the optimal designs for different types of separations.

Separation efficiency for the iDEP-Chroma devices varied from 1890 to 153,724 plates/m, which is similar to the performance obtained by microscale EK systems. For comparison, recent studies using traditional CE systems have achieved separation efficiencies in the range of 1830–11,800 plates/m for devices for protein characterization [52] and in the range of 46,000–685,000 plates/m in CE systems with EO flow modulation [53]. From Table 1, it is evident that *separation efficiency* increased with particle size, which is expected, as the DEP effects increase with particle size. Furthermore, particle charge also affects the separation efficiency, as higher magnitudes of the negative ζ_P values decrease the overall EK velocity of the particles, prolonging the interactions of the particles with the post array, leading to a higher number of plates.

Post shape optimization

After establishing a required voltage of 900 V for achieving dielectrophoretic effects and exploring correction factor values, a series of COMSOL simulations were carried out to test the effects of post shape, including post asymmetry, on the separation performance of each one of the 12 channel designs studied here (Fig. 1). The objective was identifying the channel designs that maximize the differences in retention time between the particles of interest, particles of the same size but different charges (different ζ_P), and particles of similar charge but different sizes. Different designs were chosen to observe how post asymmetry, post shape, and post horizontal separation impacted particles moving through the system. Post asymmetry can help to modify the way the particle approaches the area of the highest electric field gradient (constriction between two posts). Different post shapes form higher electric field gradient as the post shapes decrease in roundedness [20]. Post horizontal separation helps to modify the particle velocity as it moves through the system, minimizing the influence of the previous posts by increasing horizontal spacing [21]. A detailed summary of all the simulation results obtained in this study, for all 10 particles and 12 distinct channel designs, is listed in Tables S2–S5 in the ESM. Table S2 contains all raw simulation results without the use of corrections factors. ESM Table S3 contains the predicted retention times considering correction factors. ESM Tables S4 and S5 contain comparisons of particle retention time differences ($\Delta t_{R,\ e}$) for selected particle mixtures for all 12 designs aimed to identify the best designs for a separation by charge and the best design for a separation by size, respectively. Figure 3a shows a comparison of the t_R values obtained for two very similar types of particles. As listed in Table 1 (particles nos. 9 and 10), both particles are approximately 10 μm in diameter, made from polystyrene, and differ only in their particle zeta potential values (−30.8 mV vs. −72.6 mV). According to the simulation results, despite similarities between these two types of particles, the separation of a mixture of these particles is feasible employing iDEP-Chroma designs. The simulated differences in t_R values for these two types of particles range from 33.9 to 46.3 s (Fig. 3a) when 900 V is applied across the channel. Streaming iDEP allows exploiting charge differences to perform the separation of similar types of particles. The next sections will demonstrate how iDEP-Chroma also allows for separations by exploiting size differences.

Based on the results in Tables S2 and S4 (see ESM), the best design for achieving separations by charge is Oval-250-Oval-40, design no. 8 (posts shown in Fig. 1i), which is an asymmetric design with a high post length of 290 μm. The entire family of four Oval-Oval designs explored here showed great potential for iDEP separations. These results hint that post asymmetry enhances the separation process, as well as the total length of the post as shown in Fig. S1 (see ESM). The results in Tables S2 and S4 (see ESM) illustrate the asymmetric posts, with the short side toward the outlet, are the best designs that increase the discriminatory capabilities of the system by maximizing the differences in t_R. Figure 3a shows that it is feasible to separate micron-sized particles with the same size, same shape, and same type of surface functionalization and made from the same substrate material. Furthermore, for separating particles of the same size by exploiting charge differences, the Oval-250-Oval-40 showed the highest Δt_R values in general (detailed results are in ESM Table S4). Figure 3b helps to explain this phenomenon. Particles entering into the posts gradually speed up as they move along the length of the constriction, as shown by the white arrows

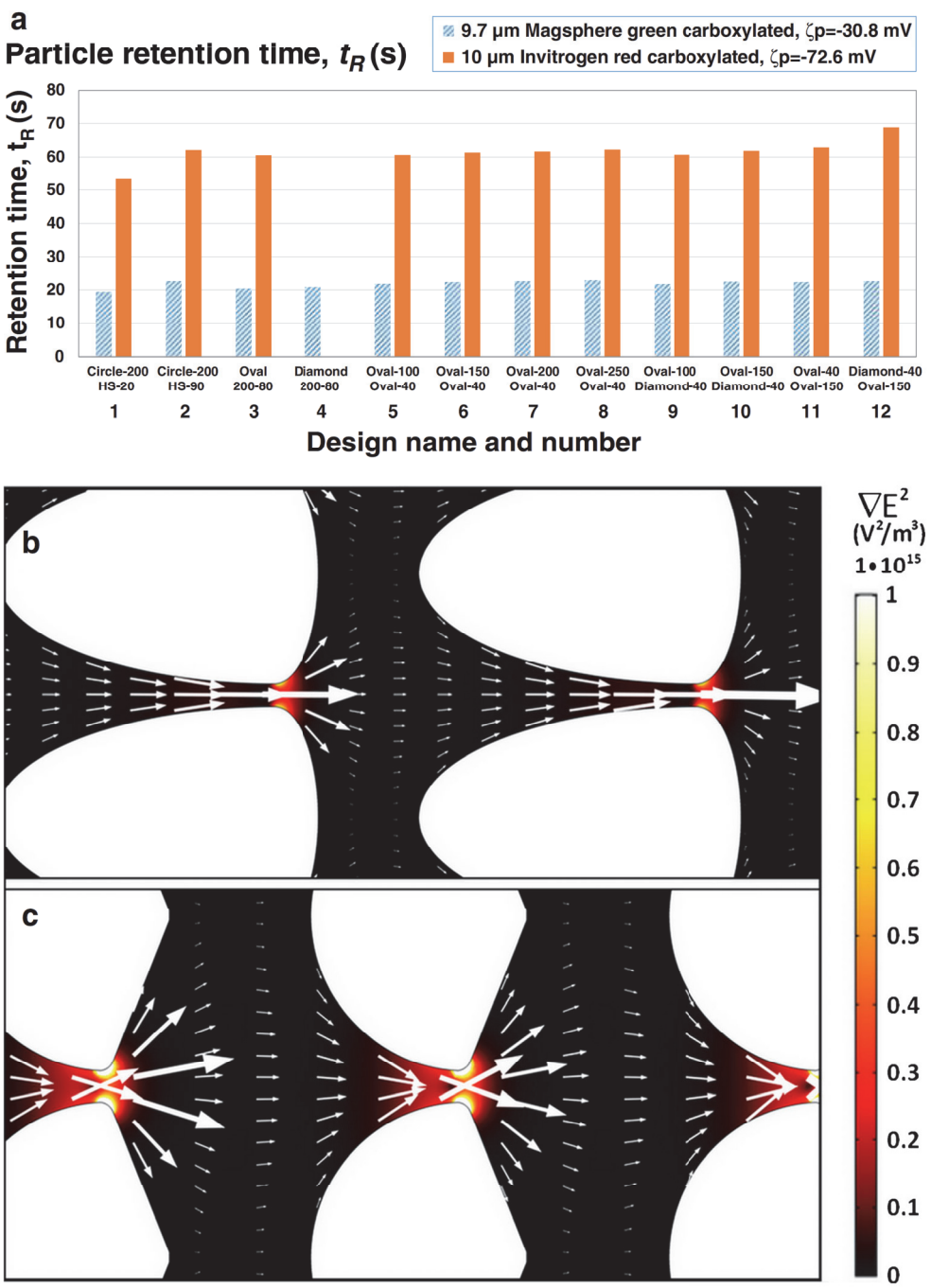

Fig. 3 (**a**) Comparison of the predicted retention time across the entire post array for two types of 10-μm particles for all designs under 900 V. These t_R values do not consider correction factors. Chosen particles are both 10 μm in diameter, polystyrene, but one is green and one is red. See particle no. 9 (green, $\zeta_P = -30.8$ mV) and particle no. 10 (red, $\zeta_P = -72.6$ mV) in Table 1. These same size and same shape particles were selected to show the potential of exploiting charge differences. Particle trapping was predicted for the 10-μm red particles in design Diamond-200-80; this value is not plotted here. (**b**) COMSOL simulation of particle velocity (arrows) and electric field gradient at 900 V obtained in Oval-250-Oval-40 design with the 10-μm red particles. This design was found to be optimized for separations by charge (see ESM Table S4). (**c**) COMSOL simulation of particle velocity (arrows) and electric field gradient at 900 V obtained in Oval-100-Diamond-40 design with the 10-μm red particles

indicating the value of the total particle velocity through the system. Particles of the same size will be subject to similar DEP force from the electric field gradient; however, the velocity at which they approach the constriction varies based on ζ_P. As particles move through the constriction, their velocity gradually increases due to conservation of mass.

Particles with greater magnitude of the negative ζ_P move more slowly through these systems, and the Oval-250-Oval-40 design presents the longest post constriction length (290 μm). Particles can move through, increasing the time before particle velocity is at the peak, marked by the smallest vertical gap between posts. The longer post design draws out the effect of the ζ_P differences between particles, having a longer constriction length which allows certain particles to fall further behind as they proceed through the constrictions. This effect is analogous to increasing the *affinity* of an analyte toward the stationary phase in chromatography, which results in the analyte interacting longer with the stationary phase.

Figure 3c demonstrates a design optimized for separations by size. When correction factors were introduced into the simulations, the Oval-200-80 (Fig. 1d), Diamond-200-80 (Fig. 1e), Oval-40-Oval-150 (Fig. 1l), and Diamond-40-Oval-150

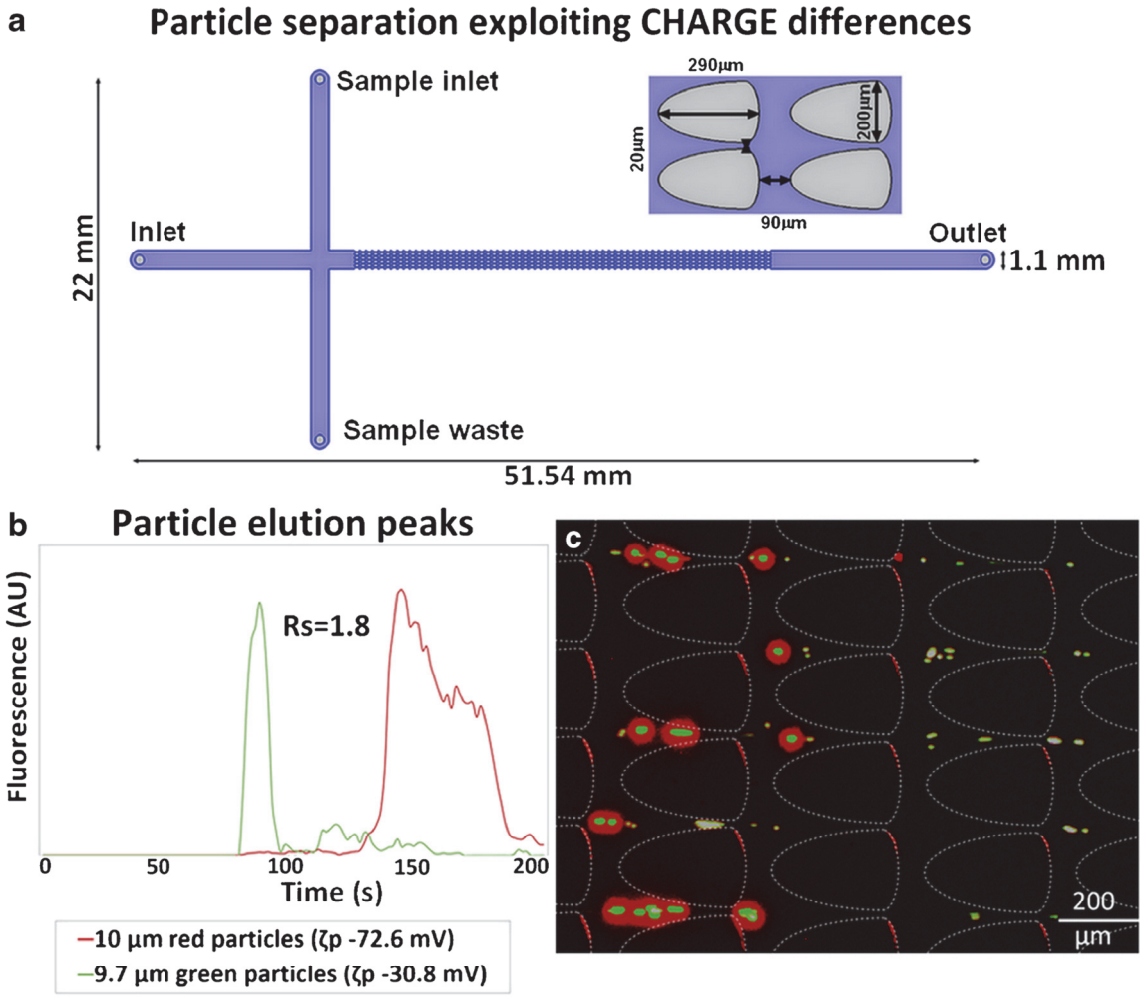

Fig. 4 Separation by charge examples in Oval-250-Oval-40 design at 1000 V. (**a**) Channel design with the post geometry inset. (**b**) Dielectropherogram and (**c**) image showing particles beginning to separate within the post array for two types of 10-µm particles; see particle no. 9 (green, $\zeta_P = -30.8$ mV) and particle no. 10 (red, $\zeta_P = -72.6$ mV) in Table 1. The dielectropherogram in (**b**) comes from Video S1 "Separation_by_charge_10um_particles.mp4" included as ESM

(Fig. 1m) designs all led to particles trapping for all available particles, as shown in Tables S3 and S5 (see ESM). Since the goal is to avoid particle trapping in iDEP-Chroma, as it is designed for streaming iDEP regime, a different design needed to be implemented. The Oval-100-Diamond-40 design gave the best potential for separation by size despite some predicted trapping for certain particles (details shown in ESM Table S5). The shorter post length allows for a maximum velocity to be reached faster, and so the pushback from DEP force directly counters the highest possible EK velocity. Smaller particles will be able to more easily maintain higher velocities as the DEP force exerted on them will be weaker while larger particles lose more velocity as they counter a higher DEP force. Furthermore, the contribution of the EK velocity at the exit of the constriction drops significantly, and so the thrust forward is less effective in the dead zone between the columns of posts, as shown by the white arrows in Fig. 3c. The sharper post design on the asymmetric Oval-100-Diamond-40 means a higher electric field gradient than the smoother oval designs, without causing particles to trap. Larger particles approaching this high gradient also have the potential to be temporarily pushed away by the high DEP force, increasing the possibility for them to interact multiple times with the constriction region before they can move through, thus increasing the retention time. Separations performed with the two optimum designs are presented in the following section.

Application: two iDEP-Chroma separations